



AALBORG UNIVERSITET
STUDENTERRAPPORT

A COMPARISON OF ADIPOSE-DERIVED STEM CELL CHARACTERISTICS BETWEEN QUANTUM EXPANSION SYSTEM AND FLASK-BASED CULTURE

Morten Brøndum Sørensen
Supervisor: Qiuyue Peng

Table of Contents

Abstract.....	3
Abbreviations:	4
1. Introduction	1
1.1 The Normal Wound Healing Process.....	1
1.1.1 Inflammatory Phase.....	1
1.1.2 Proliferation Phase	2
1.1.3 Remodeling Phase.....	2
1.2 Chronic Wound Pathology.....	2
1.3 ASCs.....	3
1.3.1 The Role of ASCs in the Healing Process	3
1.4 The Manufacturing of ASCs for Clinical Use.....	4
1.5 Multi-color Flow Cytometry	4
1.5.1 Working Principle.....	4
1.5.2 Spectrum Overlap and Compensation.....	5
2. Methods	6
2.1 SVF isolation	6
2.2 ASC Expansion.....	6
2.2.1. Culturing in Flasks	6
2.2.2. Expansion in Bioreactor.....	6
2.3 Conditioned Media Production.....	6
2.4 Scratch Assay.....	6
2.5 Tube Formation Assay	7
2.6 Proliferation Assay.....	7
2.7 CFU Assay.....	7
2.8 Tri-lineage Differentiation Assays.....	7
2.9 Multi-color Flow Cytometry	8
2.10 Data Visualization and Statistical Analysis.....	9
3 Results	10
3.1 Yields from Each Culturing Method	10
3.2 Tri-lineage Differentiation, CFU, and Proliferation.....	10
3.3 The Effect of ASC-CM on Fibroblast Proliferation and Migration	10
3.5 The Effect of ASC-CM on HDMEC Proliferation, Migration and Angiogenesis	10
4 Discussion.....	12
4.1 ASC Culturing and Proliferation after Freezing	12
4.2 Trilinear Differentiation Capacity.....	12
4.3 Immunoprofiling and Tolerance to Freezing.....	12
4.4 ASC-CM Effect on Fibroblasts and HDMECS.....	13
4.5 Tube Formation	14
5 Conclusion	14
6 Perspective	14
7 References.....	15

Abstract

Introduction: Wound healing is a complex and interconnected process where the body attempts to reestablish tissue integrity and function after injury. However, this sometimes does not happen, and the wound persists for extended periods. This is due to wounds remaining stuck in the inflammatory phase. Chronic wounds are severely detrimental to patients' quality of life. This is due to wounds remaining stuck in the inflammatory phase. Adipose-derived stem cell (ASC) based therapies have the potential to provide better treatment options. For ASC-based therapies in the chronic wound, large-scale cell production must be developed and validated.

Methods: In this study, cells cultured in a Quantum bioreactor are compared to cells cultured conventionally, in terms of surface marker profile before and after freezing, stemness, and ability to influence fibroblast and endothelial cells' migration and proliferation.

Results: No significant differences were observed between culture methods regarding stemness and ability to promote fibroblast and endothelial growth. Some surface markers, such as CD146, CD271, CD 247, CD105, CD34, and CD31 differed between the two culture methods before and after freezing. Furthermore, freezing-thawing procedure cells did not cause major changes in surface marker profiles. Cells grown in flasks were significantly more viable than cells grown in the bioreactor before and after freezing.

Conclusion: ASCs cultured in a Quantum bioreactor behave similarly to conventionally cultured ASCs. Freezing-thawing procedure will preserve more viable cells from the flask than bioreactor. This study provides more evidence for the choice of culture attachment material for the large-scale production of ASC in future treatments.

Abbreviations:

ADC: Analog-to-digital converter
ASC: Adipose derived stem cell
BM: Bone marrow
BP: Bandpass filter
CD: Cluster of differentiation
CFU: Colony Forming Unit
CM: Conditioned media
DAMP: Damage-associated molecular pattern
ECGM-MV2: Endothelial cell growth medium-MV2
ECM: Extracellular matrix
EGF: Epidermal growth factor
FC: Flow Cytometry
GMP: Good Manufacturing Practices
HGF: Hepatocyte growth factor
IFN- γ : Interferon gamma
IDO: Indoleamine 2,3-dioxygenase
ISCT: International Society for Cellular Therapy
IL: Interleukin
MMP: Matrix metalloprotease
MSC: Mesenchymal stem cell
PAMP: Pathogen-associated molecular pattern
PBMC: peripheral blood mononuclear cells
PDGF: Platelet-derived growth factor
PGE2: Prostaglandin E2
PMT: Photomultiplier tube
ROS: Reactive oxygen species
TGF- β : Transforming Growth factor- β
TIMPs: Tissue inhibitors of metalloproteinases
TNF- α : Tumor necrosing factor- α
VEGF: Vascular endothelial growth factor

1. Introduction

Wound healing is a complex and interconnected process wherein the body attempts to reestablish tissue integrity and homeostasis after injury. It involves recruitment and cooperation between numerous cell types to effectively move from open wound to new tissue. However, in some patients, this fails to occur in a timely manner. Instead, factors supporting tissue degradation and repair stay at an equilibrium, causing a chronic wound. Chronic wounds are detrimental to a patient's quality of life^{1,2} and significantly burden national healthcare systems.³ An alternative to current therapy could be switching to a cell-based therapy, specifically the use of adipose derived stem cells (ASCs) to aid wound management, as they have been shown to have positive effects on inflammation and cell proliferation.

This rapport provides an overview into how the normal wound healing process work, where it goes wrong and develops into chronic wounds, how ASCs could be useful in wound treatment, and some of the hurdles ASCs must overcome before they can move from potential in a lab setting into being a mainstay as a therapeutic option. Finally, a study is presented, wherein ASCs are cultured in a Quantum bioreactor and compared to conventionally grown cells in terms of surface marker profile and the ability to interact with fibroblasts and endothelial cells, which are crucial in wound healing.

1.1 The Normal Wound Healing Process

Wound healing is divided into four phases: Hemostasis, inflammation, proliferation, and remodeling.⁴ Hemostasis seeks to rapidly contain and counteract the damage caused by the injury. Immediate local vasoconstriction restricts blood loss, and luminal exposure of extracellular matrix (ECM) components promote platelet activation. Activated platelets upregulate the expression of surface adhesion molecules called integrins, which bind the platelets together as well as to the subendothelial ECM surrounding the wound, forming a plug. Furthermore, there is an initial burst release of growth factors, including platelet-derived growth factor (PDGF) and transforming growth factor- β (TGF- β), which all play essential roles in the following healing process.⁵ The coagulation cascade is activated, ending with circulating fibrinogen cleaving into fibrin.⁶ Fibrin then binds with the platelet plug and crosslinks with additional fibrin molecules, providing structural reinforcement. Meanwhile, Damage-associated molecular patterns (DAMP), which are intracellular proteins and molecules released from dying cells, and pathogen-associated molecular patterns (PAMP), which include bacterial lipopolysaccharides and lipoproteins, are recognized by resident immune cells. These, in turn, sound the alarm by secreting inflammatory cytokines like interleukin-1 (IL-1) and tumor necrosis factor- α (TNF- α), signaling the transition to the inflammatory phase.⁴

1.1.1 Inflammatory Phase

Cytokines activate nearby vascular endothelial cells inducing luminal expression of selectin and integrin adhesion molecules, catching circulating leukocytes, and rolling them on the vessel surface towards the injury site. When arriving at the wound, integrins tightly adhere to the leukocyte and pull it through the endothelium and basal membrane, depositing it into the interstitium. Initial response cells are neutrophils, followed by macrophages. As the neutrophils are deposited near the injury site, they sense and move toward the chemical gradient caused by DAMPs, PAMPs, and cytokines. In the wound, they phagocytose pathogens and cellular debris. Additionally, neutrophils release matrix metalloproteinases (MMPs) and reactive oxygen species (ROS) that damage microbes and digest injured tissue. The broken-up ECM fragments further act as immunostimulants, exacerbating wound inflammation.⁷ Neutrophils will be present for about two to five days, after which they undergo apoptosis and subsequent efferocytosis. Alternatively, some neutrophils escape clearance by migrating back into circulation.⁴

Macrophages enter the picture at about 72 hours. They circulate as inactive monocytes while no injury is present. As they migrate into the interstitium, they differentiate into active M1 macrophages that express IL-6, TNF- α , and IL-1 β . These have the task of phagocytosing pathogens. To aid in this objective, they also secrete MMPs that digest the surrounding ECM to move around the injury site.⁴ As the inflammation subsides, the tasks macrophages fulfill change. Newly arrived monocytes instead differentiate into their anti-inflammatory M2 configuration. These M2s play significant roles in many of the sub-steps of the proliferation phase.^{7,8}

1.1.2 Proliferation Phase

After about 72 hours post-injury, the focus begins shifting away from inflammation and towards actual wound closure.⁹ This phase consists of three co-occurring processes: fibroplasia, reepithelialization, and neovascularization. Fibroblasts from the surrounding tissue migrate to the wound in response to TGF- β and PDGF secretion. Once inside, they start proliferating as well as depositing an array of matrix proteins, including fibronectin, hyaluronan, and collagen I & III. These will provide a more permanent replacement to the fibrin clot called granulation tissue for the new blood vessels can sprout into and epidermis to grow onto.⁴ M2 Macrophages also aid in depositing matrix proteins. A subset of M2s further interacts with fibroblasts by inducing some to transition to myofibroblasts. These express α -smooth muscle actin, which gives the ability to contract in a manner similar to smooth muscle. Induced myofibroblasts migrate into the wound center, attaching to deposited fibronectin and collagen fibrils and pulling the fibrils perpendicularly to the wound edge, making the wound contract. Contracting the wound aids local keratinocytes in reestablishing the epidermis by reducing the wound area they need to cover.⁴

Reepithelialization is the process wherein the epidermis is reestablished. The epidermis comprises several layers of epithelial cells called keratinocytes, with the basal layer attached to a basal membrane. When this layer is compromised, the keratinocytes surrounding the wound will detach from the basal membrane and start expressing new integrins. These and intracellular actinomyosin filaments allow the cell to pull itself onto exposed ECM and dermis within the wound and propel itself forward. Keratinocytes around the wound edge and any hair follicle stumps that may have been left behind creep in between the dermis and the blood clot. Whenever a monolayer of keratinocyte has been reestablished, the basal lamina gets reestablished from former wound edges. Regular keratinocyte proliferation and layering occurs, finishing the new patch of epidermis.¹⁰

To supply the newly formed tissue with nutrients, new blood vessels must be formed. In response to growth factors like V vascular endothelial growth factor (VEGF), endothelial cells lining adjacent capillaries secrete proteases that digest the basal lamina surrounding them. Free to begin sprouting, the endothelial cells either take up the role of tip cells or the following stalk cells. Tip cells extend their filopodia and travel towards the pro-angiogenic gradient, guiding the new sprout forward. Meanwhile, the trailing stalk cells proliferate to maintain cell-to-cell contact between the tip cell and the original blood vessel. These will eventually start forming pinocytotic vesicles that fuse to large vacuoles inside the cells. In turn, these will also fuse, forming a continuous lumen that will ultimately become the new capillary. As in fibroplasia, M2 macrophages play a key role in angiogenesis. M2s secrete VEGF, promoting endothelial migration and proliferation. M2s also play a more direct role in capillary formation, as they have the ability to fuse the newly sprouted vessels in a process called vascular mimicry.⁴

1.1.3 Remodeling Phase

The remodeling phase intends to restore the now healed tissue to as close to the original state as possible over the following months and years. Gradual improvements of tensile strength are achieved by reorganizing, degrading, and resynthesis of the ECM. The initially deposited collagen III is disorganized and lacks tensile strength, so it is gradually degraded and replaced with stronger collagen I fibers. Myofibroblasts secrete MMPs for this task and tissue inhibitors of metalloproteinases (TIMPs) to regulate the process. Eventually, the fibroblasts start undergoing apoptosis, and their remains, along with the degraded ECM fragments, get cleaned up by resident macrophages. The newly developed blood vessels also undergo a pruning process wherein capillary density is reduced, and the remaining develop into mature blood vessels.⁴

1.2 Chronic Wound Pathology

As mentioned previously, normal wound healing is a delicate process that is supposed to end with the wound being replaced with new, functioning tissue. This, however, is not always the case. At times, wounds enter a chronic state, where the wound area will remain static or even increase in size. Chronic wounds are often seen as a late-term sequela of certain cardiovascular- or metabolic disorders such as diabetes and venous insufficiency.¹¹ Furthermore, immobilized persons can develop bedsores on pressure-bearing surfaces.¹² Experiments using fluids from acute or chronic wounds show that while adding exudate from acute wounds promotes fibroblast *in vitro* proliferation,¹³ chronic leg ulcer fluid did not.¹⁴ Indeed, experiments with exudate from chronic wounds that later were coaxed into healing show a marked inhibition of fibroblast proliferation that, in turn, reversed when using fluids from the same wound after it has entered its healing phase.¹⁵ Common among these wounds is that they remain in the inflammatory phase. Neutrophils remain present for longer than usual. This leads to an altered inflammatory profile, where excessive MMPs are released while the TIMPs and other protease inhibitors are absent.¹⁶ As a result, ECM breakdown is magnified, counteracting attempts to close the wound. The subsequent breakdown products act as proinflammatory signals to further trigger the inflammation process. Furthermore, cytokines favoring inflammation, such as TNF- α , are heavily upregulated, while growth factors like PDGF and TGF- β that are responsible for promoting proliferation and matrix deposition are severely reduced. This could be due to degradation caused by neutrophil-released elastase.^{12,17} There is also an increase in ROS excreted by neutrophils, damaging cell membranes

and ECM, promoting additional proinflammatory cytokine production.¹² All of this is complicated even further by the introduction of exogenous pathogens colonizing the open wound, exacerbating the immune response.⁸ In summary, the chronic wound is stuck in a positive feedback loop, where persistent inflammation causes tissue degradation, proinflammatory cytokine release, and anti-inflammatory cytokine degradation, which in turn induces further neutrophil infiltration and inflammation.

1.3 ASCs

Stem cells are lines of cells that can infinitely self-renewal and undergo differentiation into other cell types. Adult stem cells are multipotent, meaning that they can differentiate into select cell lines. They reside in adult tissue, supplying the body with new progenitor cells that can be differentiated into mature cells. Examples of these are the neural stem cell, which, albeit only in a limited capacity in the adult brain, generate neurons and glia, the hematopoietic stem cell, which supplies the body with red- and white blood cells; and the mesenchymal stem cell (MSC).¹⁸ MSCs are cells that, *in vivo*, can differentiate into various cell types, including myocytes, osteocytes, chondrocytes, and adipocytes.¹⁹

To standardize a common definition of MSCs, the International Society for Cellular Therapy (ISCT) has proposed three criteria: 1) plastic adhesion. 2) expression of CD105, CD73, and CD90, as well as lack of CD45, CD34, CD14, CD11b, CD79 α , CD19, and HLA-DR. 3) the ability to differentiate into osteoblasts, adipocytes, and chondrocytes *in vitro*.²⁰ MSCs are found throughout the body. Initially isolated from bone marrow (BM), they are now known to reside in joints, umbilical cords, teeth, and, most notably for this study, adipose tissue, where they are named ASCs.¹⁹ ASCs are of particular interest to researchers, as they possess most of the properties of their BM-derived cousins and offer some unique advantages that make them a more practical choice of cell line. Isolation of human BM from live patients for stem cell culturing is a complicated and arduous procedure with a severe risk of contamination, while ASC can, with relative ease, be obtained from adipose tissue waste from routine surgical and cosmetic procedures.²¹ The stem cell yield for ASCs is higher than that of BM-MSCs as well,²² making obtaining a suitable amount of donor cells for further culturing comparatively easy.

1.3.1 The Role of ASCs in the Healing Process

The exact role of ASC in the wound healing process is still to be fully mapped out. However, evidence does suggest they potentially play a role in both the inflammatory, proliferative, and remodeling phases. In the inflammatory phase, they act as immunosuppressors. Cui et al. found that ASCs cultured to both passages 2 and 5 could suppress peripheral blood mononuclear cell (PBMC) proliferation despite mitogen stimulation and suppress a mixed lymphocyte reaction assay in a dose-dependent manner. The experiment was performed in a trans well set up, meaning the interaction between ASC and lymphocytes was entirely cytokine mediated. In their case, it was found that prostaglandin E2 (PGE2) was responsible for the immunosuppression observed.²³ Delarosa et al. too found that ASCs were able to inhibit PBMC proliferation, but in their study, it was found that the inhibition was mediated by indoleamine 2,3-dioxygenase (IDO).²⁴ Furthermore, ASCs have been shown to promote the recruitment and polarization of the anti-inflammatory M2 macrophages.^{25,26}

In the proliferation phase, ASCs support angiogenesis. Human aortic endothelial cells co-cultured with ASCs showed significantly improved viability, migration, and tube formation ability *in vitro*. This was attributed to ASC VEGF and hepatocyte growth factor (HGF) secretion, as treating endothelial cells with CM, wherein VEGF and HGF were removed from the equation via neutralizing antibodies, showed significantly impaired proliferation and migration ability.²⁷ This ability to promote vascularization has also been shown in *in vivo* models, wherein ASC promoted blood vessel development in a murine ischemic limb model, where Sumi et al. showed that injecting ASCs improved blood perfusion and capillary density to the same degree as injecting BM-MSCs did.²⁸

ASCs further stimulate fibroblast migration, proliferation, and ECM synthesis *in vitro* and *in vivo*. Specifically, Cho et al. showed that CM from ASCs previously treated with TGF- β , a growth factor abundant in wounds, significantly increases fibroblast expression of MMP-1 and collagen-I as well as proliferation and migratory ability in a scratch assay. This was also investigated in an *in vivo* murine wound model, where TGF- β treated ASC-CM significantly accelerated wound healing. CM from non-treated ASCs was also effective, albeit to a lesser extent.²⁹ The mechanism of action for how ASCs exert the abovementioned effect is not fully known. However, it would seem that at least part of it is through the excretion of exosomes, as Hu et al. found that fibroblasts can absorb exosomes concentrated from ASC-CM, which promotes migration, proliferation, and collagen-1 synthesis *in vitro*.³⁰ As mentioned, fluid from chronic wounds differs in composition from fluid taken from acute wounds. Koenen et al. found it also markedly influences ASCs' behavior *in vitro*. Acute wound fluid improved ASC proliferation, as seen in other cells, and chronic wound fluid inhibited proliferation. However, chronic wound fluid stimulated ASCs to strongly secrete growth factors like basic fibroblast growth factor (b-FGF), VEGF, as well as MMP-9, something only mildly stimulated by the acute wound fluid.³¹

In the remodeling phase, ASCs have the capacity to guide fibroblast behavior in service of reducing scarring. This was shown in a murine model, wherein injecting exosomes from human ASCs decreased scarring, increasing the ratio of collagen III to I present in the wound and activating pathways that increase MMP3 presence, which is key to remodeling the ECM.³²

1.4 The Manufacturing of ASCs for Clinical Use

While ASC-based therapies show potential as a treatment paradigm, numerous hurdles remain to overcome before promising small-scale research results can be translated into clinical use on patients. Ideally, therapies using ASCs would be allogeneic rather than autologous, as this would better allow for scaling and standardizing treatment protocols while following good manufacturing practices (GMP). Autologous treatment is further encumbered by the fact that data suggest that ASCs are not a uniform resource for manufacturers to extract. Indeed, it seems that donor sex influences ASC capabilities, as Shu et al. reported significant differences in proliferative capability, growth hormone secretion, and apoptosis rate, with ASCs from females generally performing better. They further found that age had a negative effect on the abovementioned parameters.³³ Considering the fact that the chronic wound patient population tends heavily towards the elderly, cell performance being negatively correlated with age makes autologous grafts suboptimal. Moreover, ASCs from experimentally induced diabetic mice show poorer ability to support neovascularization.³⁴ When comparing three different donors in terms of wound healing, Ren et al. found that one of their donors consistently outperformed the two others in the ability to induce proliferation and migration in fibroblasts and endothelial cells as well as promote angiogenesis.³⁵ Even extraction location may be of significance. Fraser et al. showed that samples extracted from patient thighs yielded an ASC population with more osteogenic progenitors than samples from the same population's abdomen.³⁶ The heterogeneity in ASC performance may be due to different distributions of ASC subpopulations. Indeed, immunoprofiling has found several distinct populations of ASCs that show differing abilities in terms of wound healing *in vitro*.³⁷

Another key factor to consider is how cells will be produced by post-extraction. Traditionally, cells are grown in culture flasks. However, protocols from current clinical trials use millions and, in some cases, billions of cells per treatment.³⁸ This alone makes flask culturing prohibitively costly and labor intensive, especially for plastic adherent cell cultures like ASCs. Furthermore, it is quite hard to maintain homogeneity between every flask culture³⁸ and, while attempts at ensuring sterile conditions are done in cell labs, manual flask culturing necessitates exposing cell cultures to the outside environment while changing media, subculturing, etc., increasing the risk of contamination³⁹. Bioreactors were developed as an alternative to conventional culturing methods. These enable large-scale cell production while maintaining GMP compliance. In the case of the Quantum cell expansion system, the system available in our lab, cells are loaded into a disposable hollow fiber expansion chamber and left to expand on the 2.1m² surface area. Media is pumped through a sterile filter into an IV-style bag and then connected to the machine, which pumps media through the expansion chamber at a user-defined rate, depending on the number of cells present. Waste is similarly discarded into a bag, making the setup an entirely closed-loop system. The continuous flow of media also ensures the homogeneity of the cell milieu. As cell confluency cannot be directly observed, activity is instead measured using lactate and glucose concentration from an outlet port. The media feed rate is adjusted according to protocol.⁴⁰

While the Quantum has been successfully used for both expanding BM-MSCs and ASCs populations from single donors into what could be seen as industrial-scale production^{39,41-43}, more work needs to be done on ensuring that the cells produced will 'conform' to what one might expect based on smaller scale flask results. Specifically, immunophenotyping has mostly centered around identification according to the criteria set forth by ISCT, not factors that may contribute toward wound healing potential. Along the same vein, little work has been done comparing functional aspects, i.e., interactions between ASCs and target cells vital in wound healing, between cells grown in a bioreactor and those cultured conventionally.

1.5 Multi-color Flow Cytometry

1.5.1 Working Principle

Several approaches exist when examining the surface marker expression of a given cell line. Qualitative information about the existence and possible intracellular location can be found using immunocytochemistry, and *in situ* location can be found with immunohistochemistry. To do it on a large number of cells in a quantifiable and expedient manner, one turns to flow cytometry (FC). A flow cytometer generally is comprised of three main systems: Fluidics, optics, and electronics. Fluidics is the system that carries cells from the test tube and through the machine while focusing them into a neat, straight line of single cells to be measured by the machine's lasers. The sample fluid is pumped into a flow chamber, where a sheath fluid surrounds it before moving to the laser setup. This sheath fluid propels the sample fluid forward and forces it towards the center of the tubing, a principle termed hydrodynamic focusing. There is a pressure differential between the two liquids and changing this allows the user to choose the width of the sample stream, with a higher differential pressure producing a wider sample stream. Selecting a higher pressure has the advantage of increasing the number of cells coming into contact with the laser every second, speeding up the analysis. However, the wider sample stream does result in some cells not hitting the center of the laser beam, meaning their reading needs to be discarded. Conversely, a low sample pressure narrows the sample stream, reducing the number of erroneous readings, but increasing analysis time. Selecting the proper pressure for a given sample depends on how many cells one has in suspension as well as the precision needed for one's analysis. If one

has relatively few cells, lower speeds are more appropriate. Furthermore, some analyses, such as DNA content analysis, require greater resolution and must be run at lower speeds.⁴⁴

Optics is the collection of lasers, filters, and photon detectors that measure cell characteristics. Lasers with specific wavelengths of light are shined at the cells as they pass through the system. This light interacts with the cell edges and its contents and is scattered. The slight bending of light caused by the cell edges is called the forward scatter and is correlated with cell size, while the light being scattered around 90 degrees is called the side scatter and relates to the granularity of the cell. Meanwhile, if the cell has any fluorochrome-bound antibodies affixed to it, it will absorb a specific wavelength of light and emit another, lower frequency wavelength. The resulting light will then be passed through a series of dichromatic mirrors that act as filters and point the light at the appropriate detector. These mirrors can act as either short pass filters, which only let light through that is a lower frequency than specified, long pass filters, which let light through that is a higher frequency than specified, and bandpass filters, which let light through that is of a frequency between a lower and higher bound.^{44,45}

Lastly, there is the electronics. These detectors at the end of the optics setup absorb the light passed through to them and translate it into electrical signals for the machine to present as data. As the light from the emitted fluorescence hits the photomultiplier tube (PMT), a voltage spike is generated proportional to the light intensity and duration. The voltage is fed through an amplifier to an analog-to-digital converter (ADC). These assign a value to each signal based on the voltage pulse characteristics, which in turn is assigned within a certain threshold in a process called binning.⁴⁴

The level of signal amplification before digitization is configurable by the user and is a key point in analysis optimization. In a manner somewhat analogous to exposure time in light microscopy, correctly setting the PMT voltage allows dim signals to be apparent against the background while not letting bright signals get 'overexposed' and fall out of the detection range.⁴⁵

1.5.2 Spectrum Overlap and Compensation

When performing a flow cytometry experiment, one must be cognizant that fluorochromes do not get excited and emit in a binary fashion like a light switch. They will have an excitation and emission wavelength that excites them the most and of which they will emit the most light, but both points are but a maximum along a larger curve. There is, therefore, significant spillover between many fluorochromes used for FC. A classic example of this is the use of FITC and PE together. FITC has peak excitation at 491nm and peak emission at 516 nm, while PE has peak excitation at 566 nm and peak emission at 574 nm. However, as is often the case, both have a significant 'tail' on the emission spectrum after their peak. Because of this as well as their relative proximity to each other, there will be a large amount of spillover of FITC into the channel used to detect the PE signal (approximately 15-20% of the maximum found in the 525/40 band will be seen in the 585/42 band used for PE detection). While this could be negated by choosing fluorochromes with emission spectra further from each other, this rapidly becomes impossible as one continues to add additional targets to the analysis. To mitigate the amount of spectral overlap there is between one's fluorochromes, one must employ a procedure termed compensation. This involves running cells or beads stained with a single fluorochrome for every fluorochrome used. With the data, one can generate a spillover matrix from which a compensation matrix for each fluorochrome and channel can be developed and imported to one's analysis program of choice.⁴⁶(For more details on the math involved, see.⁴⁷)

2. Methods

2.1 SVF isolation

ASCs were isolated from human adipose tissue extracted from a patient undergoing an unrelated surgical procedure at Aalborg University Hospital, Aalborg, Denmark. Informed consent was sought and granted before the procedure. 30 ml adipose tissue was transferred into 500 ml conical flasks (430422, Corning, Tewksbury, MA, USA). The tissue was washed by adding 200ml of PBS to the flask, vigorously shaking the contents, and letting the contents separate into two phases. The lower phase was aspirated, and the procedure was repeated two times. 25 ml of tissue was then transferred into 50 ml centrifuge tubes. To liberate the cells from the tissue, each tube was incubated in 25 ml of collagenase mixture consisting of 10% collagenase (collagenase NB4, #S1745403, Nordmark Biochemicals, Uetersen, Germany) in 1x HBSS (#14065-049, Fisher Scientific, Roskilde, Denmark) and placed on a 37°C heated rocker for 1 h. Each tube was vacuum filtered through a 100 µm steriflip filter (SCNY00100, Millipore, Søborg, Denmark). The resulting filtrate was centrifuged at 400 x g for 10 min. The supernatant was discarded, and the pellet was resuspended in 10 ml growth media (95% α-MEM (12561056, Gibco, Roskilde, Denmark) with 5% human platelet lysate (HPL, SCM152, Millipore, Søborg, Denmark) and 1% Penicillin/Streptomycin (P/S, 15140-122, Gibco, Roskilde, Denmark). Filtration was repeated using a 60 µm filter (SCNY00060, Millipore, Søborg, Denmark) and centrifugation at 400 x g for 10 min. The resulting pellet was resuspended in 10 ml growth media and counted with an automatic cell counter (Nucleocounter NC-200, Chemometec, Allerød, Denmark). 80% of cells were set aside for bioreactor use and the rest was seeded into a T175 culture flask.

2.2 ASC Expansion

2.2.1. Culturing in Flasks

The resulting cells in the flask were cultured at 37°C for 24 h. After checking the cells under the microscope, the flask was washed with PBS twice to remove dead and non-adherent cells before adding new media. The media was changed twice a week. At 80-90% confluency (referred to as passage 1), cells were detached using 3 ml of TrypLE(12604-013, Gibco, Roskilde, Denmark). After counting the cells, they would be split into three new T175 culture flasks. The same procedure was repeated until passage 4, where one flask was used for flow cytometry analysis and the rest were frozen for later analysis.

2.2.2. Expansion in Bioreactor

For this experiment, the Quantum cell expansion system (Terumo BCT, Lakewood, Colorado, USA) was used according to the manufacturer's instructions. Briefly, a one-time-use expansion set was loaded into the machine and primed with PBS for 35 min. The expansion chamber was then coated with a fibronectin solution overnight. This was followed by adding media to the system and the eventual loading and attachment of cells over the next 24 h. After cell attachment, cells were fed 1 ml of media per minute. Daily lactate and glucose concentrations were measured, and when the lactate reached 3 mmol/l, the media feed rate was doubled. The feed rate was doubled after every subsequent 1mmol/l increase in lactate concentration until it reached 6 mmol/l, at which point the feed rate was again doubled and allowed to run for 24 h. At this point, the cells within the system were trypsinized for 30 min and extracted. Note that, regardless of lactate concentration, each step had to be run for at least 24 h and could not be skipped.

2.3 Conditioned Media Production

ASCs were seeded at 20000/cm² in T175 flasks and cultured for at least 24 h to recover from the freezing-thawing process. Afterwards, cells were trypsinized, resuspended, and re-seeded at a density of 15000/cm² in T175 flasks and allowed to proliferate until they reached 80% confluency. At that point, the cells were washed thrice, and new media was added, followed by an additional 24 h of culturing. The conditioned media was collected in 50 ml centrifuge tubes and centrifuged at 1000 x g for 15 minutes. The lactate concentration of condition media was measured using a lactate meter (Lactate Plus, Nova Biomedical, Waltham, USA) before being aliquoted into 2 ml samples and stored at -20°C for later use. Cell numbers were counted as well.

2.4 Scratch Assay

Human dermal fibroblasts (HDFs) and human dermal microvascular endothelial cells (HDMEC) were seeded into a 96-well plate at 12000 cells/cm² and cultured until HDFs reached 100% confluency. A scratch for each well was made by an auto-scratcher (AUTOSCRATCH, Agilent, Glostrup, Denmark). Each well was washed with PBS twice to remove detached cells or debris and fed with either ASC-CM from bioreactor cells, ASC-CM from flask cells, or standard growth media. To monitor the scratch closure, the plate was placed into an incubator with a time-lapse microscope (Omni, CytoSmart, Eindhoven, Netherlands). The photos were taken every 4 h for 72 h. The scratch area was calculated by a scratch assay algorithm provided by the microscope manufacturer.

2.5 Tube Formation Assay

Matrigel (E6909, Merck, Schnelldorf, Germany) was procured from the freezer the day before analysis and placed at 4°C in an ice bath overnight. Pipettes, pipette tips, PBS, and a 48-well plate were placed at 4°C as well. On the analysis day, each well needed was wetted with PBS before having 130µl Matrigel applied to coat the well bottom and set to cure at 37°C for 30 min. Meanwhile, HDMECs that were around 80% confluent were trypsinized, resuspended, and counted. 100µl of CM, α -mem growth media, or ECGM-MV2 media (C-22121, Promocell, Heidelberg, Germany) containing 20000 cells was transferred into each well. The plate was then incubated at 37°C and imaged at 2 h, 4 h, 6 h, 8h, 12 h, and 24 h using brightfield microscopy. The resulting images were processed with ImageJ using a tube formation algorithm.⁴⁸

2.6 Proliferation Assay

ASCs from both sources were seeded at 600 cells/cm² in 96-well plates and cultured with media change every four days. On days 1, 3, 5, 7, 9, 11, 13, and 15, cells were washed with PBS and lysed with 0.02% SDS. After incubating for 30 min at room temperature, the plate was securely wrapped with parafilm and stored at -20°C until further analysis. This procedure was repeated with HDFs and HDMECs growing in ASC-CM, with a seeding density of 600 cells/cm² for 13 days and 15000 cells/cm² for 5 days, respectively.

On the day of analysis, after thawing all the plates, 300 µl TE buffer was added to each well, and a complete mixture was attained with vigorous pipetting. 100 µl of each sample or DNA standard (500, 100, 50, 10, 1, and 0 ng/ml) was transferred to black 96-well plates. Following this, 100 µl of 1/200 PicoGreen (P7589, Invitrogen, Taastrup, Denmark) diluted in TE buffer was added. Plates were wrapped in tinfoil, placed on a microplate shaker for 1 min, and set to incubate for 10 mins. Fluorescence measurements were taken with a plate reader (Enspire, PerkinElmer, Boston, MA, USA) at 485 nm excitation and emission at 535 nm. Standard curves were constructed via the DNA standard using linear regression, from which the DNA contents of each sample could be calculated.

2.7 Colony Forming Unit (CFU) Assay

ASCs from both sources were seeded at 30, 10, 3, and 1 cell/well, with 24 replicates for each density. Plates were incubated at 37°C for 14 days, with media changes every four days. On the day of analysis, wells were washed twice with PBS and later fixed with 4% formaldehyde for 5 mins. Cells were then stained with 0.05% crystal violet (C6158, Sigma Aldrich, Søborg, Denmark) solution for 30 mins, after which wells were washed with 200 µl tap water twice. Positive wells of each cell concentration were tallied and analyzed with L-Calc (Stem Cell Technologies, Vancouver, BC, Canada).

2.8 Tri-lineage Differentiation Assays

For the adipogenesis and osteogenesis differentiation, ASCs were seeded into 24 well flat bottom plates at 8000 cells per well and grown to 80% confluency in standard growth media. At this point, ASCs were washed with PBS and induced with adipogenesis (A10070, Gibco, Søborg, Denmark) or osteogenesis differentiation assay (A1007201, Gibco, Søborg, Denmark), while the control cells were continued to be fed by standard growth media. After an incubation period of 7 and 21 days, respectively, cells were moved to the staining procedure. Cells were fixed with 4% formaldehyde for 30 mins. Adipocytes were stained with Oil Red O (o1391, Sigma Aldrich, Søborg, Denmark) for 1h. Osteoblasts were stained with Alizarin Red S (LAB44847.1000, BB Gruppen, Denmark) for 3 min. After washing 3 times with distilled water, cells were examined with light microscopy (CKX41, Olympus life science, Ballerup, Denmark) and a Pixelink camera (PL-A782, Gloucester, Canada).

For chondrogenesis analysis, ASCs of both origins were seeded at 80000 cells/well in either chondrogenesis differentiation media (A10071-01, Gibco, Søborg, Denmark) or standard growth media into a 96 v-bottom well plate. The plate was then centrifuged at 500 x g for 5 minutes and incubated at 37°C. Media was changed every three to four days. After 21 days of induction, the pellets were collected and placed in a tissue cassette. These pellets were fixed in 4% formaldehyde for 18 h, followed by a series of dehydration steps. Pellets were then embedded in paraffin and cut into 5 µm sections. After deparaffinization, the sections were stained with alcian blue (RRSP4-D, Atom Scientific, Hyde, UK) for 30 min and hematoxylin for 1 min. Finally, each slide was mounted by with Pertex(00801, Histolab, Göteborg, Sweden) and imaged by upright brightfield microscopy (Observer Z1, Zeiss, Birkerød, Denmark),

2.9 Multi-color Flow Cytometry

Cells were stained with antibodies against CD248(743899), CD200(563254), CD166(742373), CD146(564327), CD34(560710), CD274(565188), CD271(564580), CD201(743552), CD36(563518), CD29(743785), CD31(563653), CD105(563264), CD73(561254), and CD90(561557) (BD Bioscience, Lyngby, Denmark), and STRO-1(FAB1038R, RnD Systems, Abingdon, UK). These surface markers and their corresponding fluorochromes were divided into three panels (Table 1-4). As for the experimental setup, cells were initially stained with FVS570(2869635, BD Bioscience, Lyngby, Denmark) for 15 min at room temperature, followed by a batch of antibody cocktail for 30 min at 4°C with slight agitation. The optimal concentration of each antibody was based on previous titration experiments. Settings for each experimental tube were listed in Tables 2, 3, and 4. FMO controls were applied. The cells were analyzed on a flow cytometer Cytoflex (Beckman Coulter, Copenhagen, Denmark), and the resulting data was further analyzed using the Kaluza 2.1 software package (Beckman Coulter, Copenhagen, Denmark). The top 2% of FMO control was regarded as positive.

Table 1: Panel design of fluorescent antibodies

Laser	Channel	Dye	Panel 1	Panel 2	Panel 3
405nm	450/45 BP	BV421	CD248	CD201	
	525/40 BP	BV510	CD200		CD105
	610/20 BP	BV605	CD166	CD36	
	660/20 BP	BV650		CD29	
488nm	525/40 BP	FITC/BV515	CD271		CD73
	690/50 BP	Percp-cy5.5			CD90
561nm	610/20 BP	PE-CF594	CD146		
	585/42 BP	PE	FVS570	FVS570	FVS570
	780/60 BP	PE-Cy7	CD34		
638nm	660/20 BP	Alexaflour647		STRO-1	
	712/25 BP	APC-R7000	CD274		
	780/60 BP	APC-Cy7		CD31	

NB: FITC was conjugated onto the CD73 antibody and BV515 on the CD271 antibody. BP: bandpass. CD: cluster of differentiation

Table 2: Experimental setting for each sample tube for Panel 1

Tube name	CD248- BV421	CD200- BV519	CD166- BV605	CD271- BV515	CD146-PE- CF594	CD34- PE-Cy7	CD274- APC-R7000	FVS570- PE
unstained	-	-	-	-	-	-	-	+
CD248-FMO	-	+	+	+	+	+	+	+
CD200-FMO	+	-	+	+	+	+	+	+
CD166-FMO	+	+	-	+	+	+	+	+
CD271-FMO	+	+	+	-	+	+	+	+
CD146-FMO	+	+	+	+	-	+	+	+
CD34-FMO	+	+	+	+	+	-	+	+
CD274-FMO	+	+	+	+	+	+	-	+
Full stain	+	+	+	+	+	+	+	+

Table 3: Experimental setting for each sample tube for Panel 2

Tube name	CD201-BV421	CD36-BV605	CD29-BV650	STRO-1-AF647	CD31- APC-Cy7	FVS570-PE
Unstained	-	-	-	-	-	+
CD201-FMO	-	+	+	+	+	+
CD36-FMO	+	-	+	+	+	+
CD29-FMO	+	+	-	+	+	+
STRO-1-FMO	+	+	+	-	+	+
CD31-FMO	+	+	+	+	-	+
Full stain	+	+	+	+	+	+

Table 4: Experimental setting for each sample tube for Panel 3

Tube name	CD105-BV510	CD73-FITC	CD90-Percp-cy5.5	FVS570-PE
Unstained	-	-	-	+
CD105-FMO	-	+	+	+
CD73-FMO	+	-	+	+
CD90-FMO	+	+	-	+
Full stain	+	+	+	+

2.10 Data Visualization and Statistical Analysis

Data is presented as mean \pm standard error of mean. To examine any statistically significant difference between groups in the ASC proliferation assay, a Student's paired T-test was performed. To determine if there were statistically significant differences in the HDF and HDMEC migration- and proliferation assays, a one-way repeated measures ANOVA with Bonferonni post hoc was performed. To determine if there was any statistically significant difference between groups with respect to viability, a one-way ANOVA with Bonferonni post hoc was performed. A result is considered significant if $P < 0.05$. All statistical tests were performed using SPSS.

3 Results

3.1 Yields from Each Culturing Method

Culturing cells in the Quantum bioreactor took 15 days. The initial cell load was 14.9 million cells, yielding about 39 million cells. Using the population doubling formula $PD = 3.32 (\log X_e - \log X_b)$, the result is 1.4. Flasks were initially seeded with 3.7 million cells, with an end yield of 9.3 million cells and a PD of 1.3.

3.2 Tri-lineage Differentiation, CFU, and Proliferation

Representative images of the tri-lineage differentiation can be seen in Figure A. Cells from both flask and bioreactor show differentiation into mature adipocytes, characterized by their large, round shape with lipid droplets that are stained by oil red O. Cells grown in standard growth media as a control do not exhibit any morphological changes, exhibiting no ability for lipid accumulation and storage. Similarly, osteogenesis cultures show marked positivity for calcium depositing, as shown by Alizarin Red S staining. Control cultures show no noticeable red staining. For chondrogenesis, cultures grown in chondrocyte differentiation media displayed a better ability for pellet formation than controls and positivity for glycosaminoglycans deposits, as shown by alcian blue staining. Control cultures showed limited pellet formation in culture wells and no detectable staining. (Figure A) For the CFU analysis, 13% of cells from bioreactor cells displayed colony-forming potential, which is similar to the flask cells' 14%. Over a 15-day period, there was no significant difference in proliferation between cells grown in a bioreactor versus conventional techniques ($P=0.180$) (Figure B). Growth continues for 13 days, after which a steep decline is seen in both groups.

3.3 The Effect of ASC-CM on Fibroblast Proliferation and Migration

As for the proliferation, both types of conditioned media were significantly outperformed by the control group ($P<0.001$). There was no statistically significant difference between the two test groups ($P=0.544$). (Figure C).

Conditioned media from the flask and bioreactor-grown cells significantly stimulated fibroblast migration compared to the control group ($P<0.001$). There was, however, no statistically significant difference between the two test groups ($P=1$) (Figure D).

3.5 The Effect of ASC-CM on HDMEC Proliferation, Migration and Angiogenesis

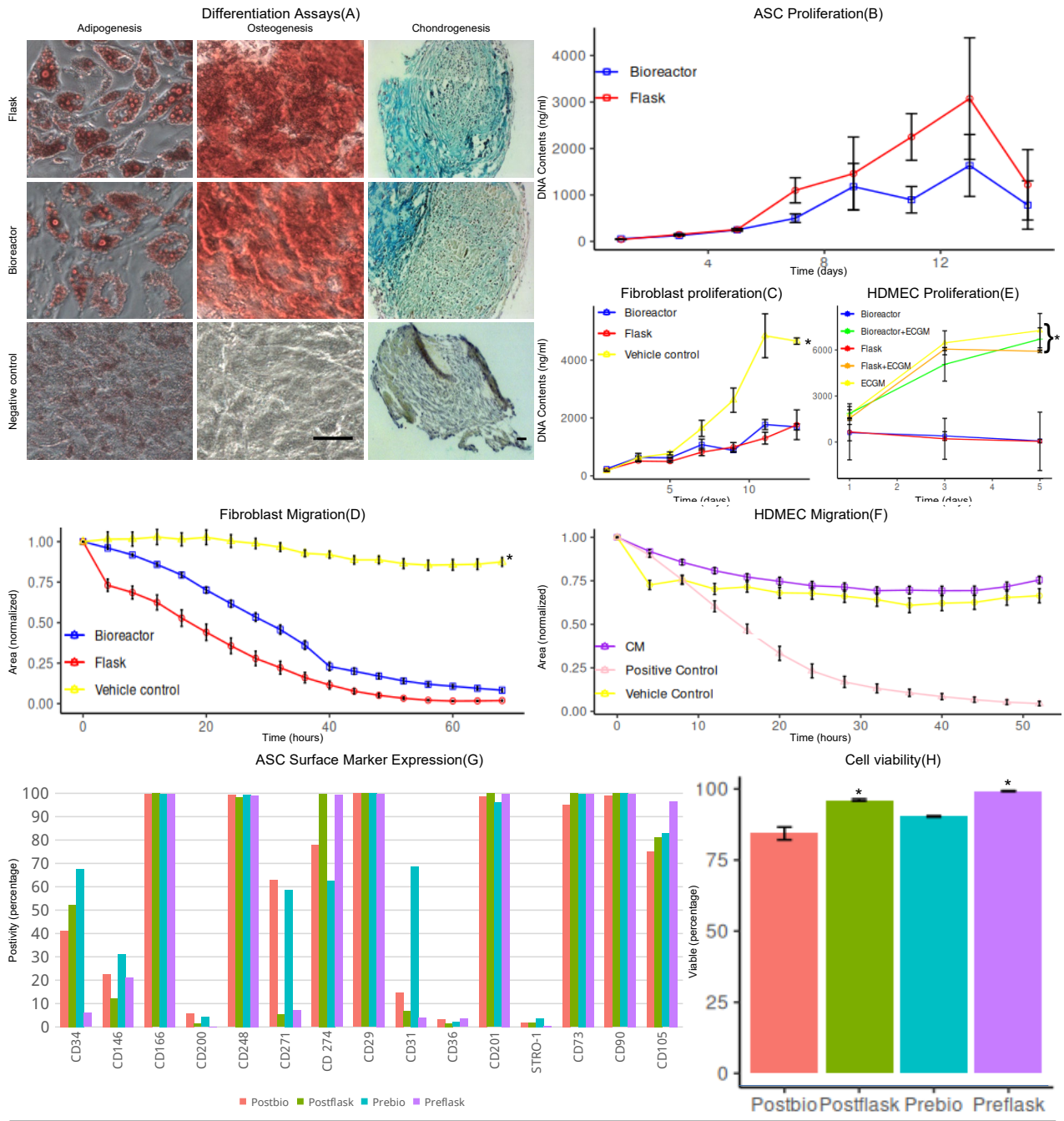
HDMECs were not able to survive in ASC-CM alone. Therefore, a mix of 50% ECGM-MV2 and 50% conditioned media harvested from both sources was prepared. These, as well as the positive control, significantly outperformed the pure CM groups ($P<0.001$). there was no statistical difference between the 50%bioreactorCM, 50%flaskCM, and the positive control ($p=1$). There was also no statistically significant difference between the pure bioreactor CM and flask CM ($p=1$) (Figure E)

The formal migration assay using conditioned media from the bioreactor and flask ASCs was unsuccessful due to hardware failure and time constraints. However, pre-experimental data suggests that it might not have worked regardless, as attempts using separately made, fresh flask CM did not generate any difference between the CM and the vehicle control. The vehicle control and CM stabilized at around 75% of the scratch still being there, whereas the positive control group closed the scratch entirely. (Figure F)

Attempts to get the tube formation assay to work correctly were unsuccessful. An initial run using CM and positive control yielded some results. However, as we did further experiments, not even the positive control was able to produce any vessel structures. (Appendix A)

3.7 Surface Marker Profiling, Frost Tolerance, and Cell Viability

Expression levels of CD166, CD248, CD29, CD201, CD73, and CD90 exhibit near universal expression, while CD36, CD 200, and STRO-1 have minimal expression in all groups. CD146 has a low to moderate expression in both cell types, with approx. 10%-point higher expression in bioreactor cells both pre- and post-freeze. CD 271 is markedly higher expressed in bioreactor cells with an approximate 50%-point difference between them and flask cells. Both CD 274 and CD105 show high expression levels, with a moderately higher expression in flask cells compared to bioreactor cells. Lastly, there are CD34 and CD31, which both vary wildly. CD34 has a moderate to high expression in bioreactor cells pre-freeze, post-freeze, and flask post-freeze. However, only 6% of pre-freeze flask cells express CD34. CD31 also has a large outlier, where pre-freeze bioreactor cells have a markedly higher expression than the rest of the test groups, which hover around $10\pm 5\%$. (Figure G & Table 4) Disregarding the two abovementioned outliers, freezing and thawing the cells had either of three effects. Either it did nothing, as with CD166, CD200, CD248, CD271, CD29, CD36, CD201, STRO-1, CD73, and CD90. Alternatively, it caused a minor decrease in expression of approx. 10%points, as is the case with CD146 and CD105. Lastly, there is CD274, where freezing increased expression by 15.08%points in bioreactor cells. This upwards trend might also be seen in flask cells, were it not for them already sporting universal expression. (Figure G & Table 4) Staining with FVS570 viability dye shows that flask cells were significantly more viable than bioreactor cells both before and after freezing ($P=0.003$ & $P<0.001$ respectively) (Figure H & table 5)



(5)

	CD34	CD146	CD166	CD200	CD248	CD271	CD274	CD29	CD31	CD36	CD201	STRO	CD73	CD90	CD105	Viability
Preflask	4.79	20.66	99.82	0.04	99.02	5.68	99.13	99.93	3.41	3.05	99.94	0.27	99.81	99.90	96.75	99.25 ± 0.11
Postflask	53.75	11.92	100	1.10	97.64	3.94	99.65	99.76	24.69	5.58	99.18	2.77	96.53	99.64	70.90	96.09 ± 0.36
Prebio	60.31	30.45	99.65	4.08	99.37	58.39	59.88	100	76.89	3.14	94.71	3.28	97.88	99.09	71.07	90.33 ± 0.17
Postbio	34.98	18.46	99.67	4.85	99.02	59.83	72.64	99.93	40.15	6.06	95.41	2.06	95.07	99.06	75.09	84.35 ± 2.23

(A) Representative images showcasing adipogenic, osteogenic, and chondrogenic abilities. Scale bar: 100µm (B) ASC proliferation over time. (n=5) (C) Fibroblast proliferation in ASC-CM over time. (n=6) (D) HDMEC proliferation in ASC-CM, 50%ASC-CM+50%ECGM-MV2, and ECGM-MV2 over time (n=3) (E) Fibroblast migration in ASC-CM. (n=5) (F) HDMEC migration in ASC-CM. (n=5) (G) Surface marker profile of bioreactor and flask cells before and after freezing. Presented as a percentage of positive live, singlet cells. (n=1) (H) Cell viability as measured by lack of FV570 uptake in bioreactor and flask cells before and after freezing. (n=3) (5) Table showcasing surface marker profile of cells from both culturing methods before and after freezing as well as percentage of viable cells ± SEM. * denotes significance. Abbreviations: CD: Cluster of Differentiation. CM: Conditioned media. ECGM-MV2: Endothelial cell growth media-MV2. "X+ECGM": CM containing 50% ECGM. HDMEC: Human dermal microvascular endothelial cells. Prebio: Bioreactor grown cells before freezing. Preflask: Flask grown cells before freezing. Postbio: Bioreactor grown cells after freezing. Postflask: Flask grown cells after freezing

4 Discussion

This study examined potential differences between ASCs grown in a Quantum bioreactor versus conventional flasks. It was found that the two culturing methods were similar in terms of tri-lineage differentiation, CFU capacity, and proliferation after a freeze-thaw cycle. Furthermore, CM from both were able to significantly outperform the control group in the fibroblast migration assay. No statistical difference was detected between them in fibroblast migration test and there was no significant difference between them in either of the proliferation assays. However, yield for the bioreactor run was lower than expected and cells were significantly less viable than those grown in flasks. For the surface profile, CD166, CD248, CD29, CD201, CD73, CD90, CD36, CD200, and STRO-1 were found to have comparable levels, while other markers, such as CD146, CD271, CD247, CD105, CD34, and CD31 showed a remarkable variation between culturing methods.

4.1 ASC Culturing and Proliferation after Freezing

When culturing ASCs in the Quantum bioreactor, the number of cells produced was 39 million from a starting point of 14.9 million cells over 15 days. This was lower than expected and not the experience reflected in the literature. Other groups have managed five to ten-fold increases in cell number over 5-17 days of various MSCs, including ASCs.⁴² Those results are also more in line with previous experience from our group, where previous runs averaged a 5.8-fold increase over 8,5 days (data not shown). It was noted that when extracting the cells and being prepared for freezing, the cell suspension contained large amounts of brownish-white debris not previously observed. The sample port was also clogged halfway through the run. Clearly, something happened inside the expansion chamber that caused cells to slough off or prevented proliferation in the first place. We are unsure as to the reason this occurred. Regardless, neither test group significantly outperformed the other in the proliferation assay on the ASCs post-culturing and freezing. As Figure B suggests, however, each group had large outliers. Large outliers are problematic, as they violate the assumptions behind the paired t-test.

4.2 Trilinear Differentiation Capacity

Differentiation assay shows that cells grown in either the quantum bioreactor or flask can clearly differentiate themselves into adipocytes, osteoblasts, and chondrocytes. This indicates that it is indeed ASCs being examined and that they have their 'stemness' features intact. Along the same vein, CFU capacity was comparable between the two culturing methods. A limitation of the differentiation capacity method is the lack of quantitative results it generates. It could be that bioreactor cells are better at differentiating into adipocytes, for example. It could therefore be of interest to quantify differentiation capacity. This could be done as a variation of the CFU assay as used by Fraser et al.³⁶ Alternatively, staining of cells could be compared as done by Anderson et al., where spectrophotometry was used to quantify adipogenic capacity and calcium deposits in osteoblast cultures were analyzed using imaging software.⁴⁹

4.3 Immunoprofiling and Tolerance to Freezing

After performing surface marker profiling on cells from each culturing method, the results showed that CD166, CD248, CD29, CD201, CD73, CD90, CD36, CD200, and STRO-1 expression levels were comparable. CD146, CD271, CD274, CD105, CD34, and CD31 had differing expression levels.

CD146 is a cell adhesion molecule. Of interest to this study, it has been investigated as an MSC marker and its expression has been correlated with heightened colony-forming capacity and differentiation ability *in vitro*.⁵⁰ Furthermore, CD146+ enriched subpopulations have been shown to induce better cartilage repair and immunomodulation *in vivo* in a rat model.⁵¹ Cartilage aside, these are all desirable traits when considering ASC for wound care, so the higher expression on bioreactor cells could be a point in their favor. Another potential marker for MSCs is CD 271, a nerve growth factor receptor.⁵² ASC expression seems to be transient, as subsequent cultured cells are markedly lower in CD 271 expression.⁵³ Indeed, Quirici et al. reported that, while they were able to identify a CD271+ ASC subpopulation at the time of extraction, the expression had all but disappeared from cultured cells at week 5.⁵⁴ However, while the cells from the two culturing methods should be the same 'age', the expression on bioreactor cells are markedly higher than on those cultured in flasks. As the others also cultured their cells in flask post-extraction and saw lowered CD271 expression, this could suggest that CD271 positivity is somehow better preserved in the bioreactor. Ren et al. expanded cells from three donors using the same bioreactor setup as this study and found variability in CD271 expression, with one donor showing 60% positivity and the rest in the mid-20s.³⁵ Clearly, CD271 seems to be a highly variable surface marker in ASCs that warrants closer examination.

CD274, or Programmed death-ligand-1, is an immune regulatory protein investigated for its role in modulating T cell activation. Studies suggest that it may be linked to obesity and overexpression of CD274 plays a part in T cell dysfunction.⁵⁵ This study found a markedly higher expression of CD274 in flask cells than in bioreactor cells. Due to the negative effect of CD274 on the immune response, our result supported that bioreactor could be a favorable culturing method to select 'well-behaved' cells. More research investigating the relationship between BMI and CD274 expression and associated outcomes is warranted.

CD105 is part of the TGF- β receptor complex. It is one of the markers set forth by the ISCT in their definition of MSCs. One would therefore expect universal expression in groups, but this is not the case here, as both bioreactor groups and the post-freezing flask group show only about 75% positivity. The two other hallmark markers, CD73 and CD90, are fully expressed in all groups. It could be that there exists a subpopulation of CD105⁻ ASCs. This is not a novel concept, as Anderson et al. found murine ASCs that were CD105⁺ and CD105⁻. Moreover, the expression or lack thereof was correlated with ASC differentiation capabilities, as the CD105⁻ subpopulation was more prone to undergo adipogenesis and osteogenesis than the CD105⁺ cells.⁴⁹ This was confirmed in human ASCs by Levi et al., who also linked the increased osteogenic potential to reduced TGF- β signaling in the CD105⁻ subpopulation.⁵⁶ It could be that the bioreactor is better at preserving this subpopulation. Alternatively, it could be that the flask is better at preserving a unique CD105⁺ subpopulation that also happens to be very sensitive toward freezing.

CD34 is moderately expressed in three test groups. If one looks at the ISCT definition of MSCs, a complete lack of CD34 expression is required. Again, there is controversy in the literature about this requirement. Detection of CD34⁺ ASCs has been reported previously in early passages with subsequent loss of expression as passage number increases.^{57,58} This would be a reasonable explanation as to why the groups do not live up to the standard, as they would both be considered early passages. However, it does not explain why passage 4 flask-grown cells have minimal CD34 expression prior to freezing yet somehow 'regrow' marker expression to the same level as the bioreactor after being frozen and thawed. A likely explanation for this is operator error.

Lastly, there are the CD31 results. CD31 is another cell adhesion molecule.⁵⁹ Pre-freeze bioreactor cells are markedly higher than the post-freeze group. This relationship is not replicated in the flask cells, where pre-freeze and post-freeze hover around 5% expression. This would then suggest that the pre-freeze bioreactor result be another anomalous result due to operator error. However, the post-freeze bioreactor cells express CD31 at a higher rate than both flask samples, so there may indeed be an actual difference in expression between the two culture methods. Given the nature of the experimental setup, it was not possible to reattempt measuring the cells before they were frozen.

Throughout the freezing-thawing procedure, the expression levels of the selected markers did not show any marked differences between the two culture methods. Their expression levels either remain stable or suffer a minor decrease. One marker, CD247, bucks the trend and increases its expression level in bioreactor cells after freezing. It is unclear why this increase happened. It could be a response to stress from freezing. As the direct comparison, the flask cells, already had total expression before freezing and continued to do so afterwards, it is hard to tell. CD34 and CD31 seem to be affected by operator error. CD247 and operator errors aside, these results bode well for the possibility of building ASC cell banks as part of allogenic therapies, as cell characteristic stability is essential for building the large biobanks necessary for on-demand treatment. Although, more work would have to be done to investigate CD247s' tolerance to freezing.

Another important trait for building biobanks is that the cells are tolerant of deep freezing. This experiment found that flask cells were statistically more viable than the bioreactor cells both before and after freezing. Given the poor performance of the bioreactor when it came to culturing the cells, this is perhaps not shocking. A saving grace for the bioreactor is that it still came out as having approx. 85% viable cells post-freezing. This happens to be higher than the minimum standard for cell viability used for cell therapies, where $\geq 70\%$ is acceptable for cryopreserved products.⁶⁰ Still, procedures for decreasing viability loss during freezing should be further investigated and optimized for potential use in industry.

4.4 ASC-CM Effect on Fibroblasts and HDMECS

The investigation ASCs' ability to influence the proliferation and migration of cells critical to wound healing through paracrine secretion of growth factors did not find statistically significant differences between the CMs in any of the assays attempted. However, this should be viewed in the context of both proliferation assays ending up with negative results, wherein the CM did not work at all without supplementing with specialty media or was worse than the control. Additionally, what can be gleaned from the pre-experimental data of the HDMEC migration assay suggests that neither ASC-CM would have been successful compared to the vehicle control. This contradicts the literature, wherein ASC-CM has been successfully used to promote cell proliferation and migration.^{35,37} One positive result came from the fibroblast migration assay, where the bioreactor and flask group significantly outperformed the control group. A factor separating the fibroblast migration test from the fibroblast and HDMEC proliferation assays is that it used a later separate batch of CM generated after the initial one had been used. It could be that some unknown error had occurred when production of the first batch of CM, rendering it inert. Subsequent tests with the later batch could generate results in line with the literature. However, this does not account for the inability to generate a positive effect during the HDMEC pre-experiments. CM for these was produced in the exact same manner as for the formal experiments. Assuming that repeating the experiments yields the same results, it would be interesting to investigate what constituent parts of the CM differ. Experiments have previously been done examining which parts of the CM contribute to its positive effects. Comparing CM from cells that successfully induced proliferation versus CM that did not could highlight differences predisposing certain populations to aberrant healing.

4.5 Tube Formation

The angiogenesis experiments ended up failing to produce results. We are unsure why the Matrigel stopped working over time. (Appendix A) the gel was stored as instructed by the manufacturer and several protocols (well plate size, amount of Matrigel, cell concentration) were attempted, but to no avail. Perhaps there is some volatility in the gel production method that can render some batches better performing than others.

5 Conclusion

In conclusion, ASCs cultured in a Quantum bioreactor behave similarly to conventionally cultured ASCs in terms of stemness, proliferation, and ability to induce fibroblast migration. A majority of surface markers are expressed at the same rate, and those that are different may indeed be beneficial for bioreactor cells in later therapeutic use. Furthermore, freezing cells for later use did not cause major changes in surface marker profiles. Flask cells performed better in terms of viability, but bioreactor cells were still sufficiently viable for current manufacturing standards.

6 Perspective

The experiments done in this study have mainly focused on ASCs' ability to modulate the behavior of cells involved in the proliferation phase of wound healing. As mentioned in the introduction, a central issue in wound chronification is remaining stuck in the inflammatory phase. A future examination of bioreactor cultured cells should therefore determine their immunomodulating abilities. Specifically, it would be of great interest to validate the potential of promoting M2 macrophage recruitment as has been done previously in a flask setting.

7 References

1. Madsen UR, Hyldig N, Juel K. Outcomes in patients with chronic leg wounds in Denmark: A nationwide register-based cohort study. *Int Wound J*. 2022;19(1):156-168. doi:10.1111/iwj.13607
2. Jeffcoate WJ, Chipchase SY, Ince P, Game FL. Assessing the outcome of the management of diabetic foot ulcers using ulcer-related and person-related measures. *Diabetes Care*. 2006;29(8):1784-1787. doi:10.2337/dc06-0306
3. Nussbaum SR, Carter MJ, Fife CE, et al. An Economic Evaluation of the Impact, Cost, and Medicare Policy Implications of Chronic Nonhealing Wounds. *Value Health*. 2018;21(1):27-32. doi:10.1016/j.jval.2017.07.007
4. Rodrigues M, Kosaric N, Bonham CA, Gurtner GC. Wound Healing: A Cellular Perspective. *Physiol Rev*. 2019;99(1):665-706. doi:10.1152/physrev.00067.2017
5. Golebiewska EM, Poole AW. Platelet secretion: From haemostasis to wound healing and beyond. *Blood Rev*. 2015;29(3):153-162. doi:10.1016/j.blre.2014.10.003
6. Smith SA, Travers RJ, Morrissey JH. How it all starts: Initiation of the clotting cascade. *Crit Rev Biochem Mol Biol*. 2015;50(4):326-336. doi:10.3109/10409238.2015.1050550
7. Sindrilaru A, Scharffetter-Kochanek K. Disclosure of the Culprits: Macrophages-Versatile Regulators of Wound Healing. *Adv Wound Care (New Rochelle)*. 2013;2(7):357-368. doi:10.1089/wound.2012.0407
8. Landén NX, Li D, Ståhle M. Transition from inflammation to proliferation: a critical step during wound healing. *Cell Mol Life Sci*. 2016;73(20):3861-3885. doi:10.1007/s00018-016-2268-0
9. Velnar T, Bailey T, Smrkolj V. The wound healing process: an overview of the cellular and molecular mechanisms. *J Int Med Res*. 2009;37(5):1528-1542. doi:10.1177/147323000903700531
10. Martin P. Wound healing--aiming for perfect skin regeneration. *Science*. 1997;276(5309):75-81. doi:10.1126/science.276.5309.75
11. Chen WYJ, Rogers AA. Recent insights into the causes of chronic leg ulceration in venous diseases and implications on other types of chronic wounds. *Wound Repair Regen*. 2007;15(4):434-449. doi:10.1111/j.1524-475X.2007.00250.x
12. Diegelmann RF, Evans MC. Wound healing: an overview of acute, fibrotic and delayed healing. *Front Biosci*. 2004;9:283-289. doi:10.2741/1184
13. Schäffer MR, Tantry U, Ahrendt GM, Wasserkrug HL, Barbul A. Stimulation of fibroblast proliferation and matrix contraction by wound fluid. *Int J Biochem Cell Biol*. 1997;29(1):231-239. doi:10.1016/s1357-2725(96)00136-7
14. Mendez MV, Raffetto JD, Phillips T, Menzoian JO, Park HY. The proliferative capacity of neonatal skin fibroblasts is reduced after exposure to venous ulcer wound fluid: A potential mechanism for senescence in venous ulcers. *J Vasc Surg*. 1999;30(4):734-743. doi:10.1016/s0741-5214(99)70113-8
15. Trengove NJ, Bielefeldt-Ohmann H, Stacey MC. Mitogenic activity and cytokine levels in non-healing and healing chronic leg ulcers. *Wound Repair Regen*. 2000;8(1):13-25. doi:10.1046/j.1524-475x.2000.00013.x
16. Menke NB, Ward KR, Witten TM, Bonchev DG, Diegelmann RF. Impaired wound healing. *Clin Dermatol*. 2007;25(1):19-25. doi:10.1016/j.clindermatol.2006.12.005
17. Yager DR, Zhang LY, Liang HX, Diegelmann RF, Cohen IK. Wound fluids from human pressure ulcers contain elevated matrix metalloproteinase levels and activity compared to surgical wound fluids. *J Invest Dermatol*. 1996;107(5):743-748. doi:10.1111/1523-1747.ep12365637
18. Lanza R, Atala A. *Handbook of stem cells Volume 2, Adult and fetal stem cells*. 2nd ed. Elsevier / AP; 2012
19. Ding D, Shyu W, Lin S. Mesenchymal stem cells. *Cell Transplant*. 2011;20(1):5-14. doi:10.3727/096368910X
20. Dominici M, Le Blanc K, Mueller I, et al. Minimal criteria for defining multipotent mesenchymal stromal cells. The International Society for Cellular Therapy position statement. *Cytotherapy*. 2006;8(4):315-317. doi:10.1080/14653240600855905
21. Fathi E, Farahzadi R. Isolation, Culturing, Characterization and Aging of Adipose Tissue-derived Mesenchymal Stem Cells: A Brief Overview. *Brazilian Archives of Biology and Technology*. 2016;59
22. Hassan WU, Greiser U, Wang W. Role of adipose-derived stem cells in wound healing. *Wound Repair Regen*. 2014;22(3):313-325. doi:10.1111/wrr.12173
23. Cui L, Yin S, Liu W, Li N, Zhang W, Cao Y. Expanded adipose-derived stem cells suppress mixed lymphocyte reaction by secretion of prostaglandin E2. *Tissue Eng*. 2007;13(6):1185-1195. doi:10.1089/ten.2006.0315
24. DelaRosa O, Lombardo E, Beraza A, et al. Requirement of IFN-gamma-mediated indoleamine 2,3-dioxygenase expression in the modulation of lymphocyte proliferation by human adipose-derived stem cells. *Tissue Eng Part A*. 2009;15(10):2795-2806. doi:10.1089/ten.TEA.2008.0630
25. Manning CN, Martel C, Sakiyama-Elbert SE, et al. Adipose-derived mesenchymal stromal cells modulate tendon fibroblast responses to macrophage-induced inflammation in vitro. *Stem Cell Res Ther*. 2015;6(1):74-4. doi:10.1186/s13287-015-0059-4
26. Mazini L, Rochette L, Admou B, Amal S, Malka G. Hopes and Limits of Adipose-Derived Stem Cells (ADSCs) and Mesenchymal Stem Cells (MSCs) in Wound Healing. *Int J Mol Sci*. 2020;21(4):1306. doi: 10.3390/ijms21041306. doi:10.3390/ijms21041306
27. Nakagami H, Maeda K, Morishita R, et al. Novel autologous cell therapy in ischemic limb disease through growth factor secretion by cultured adipose tissue-derived stromal cells. *Arterioscler Thromb Vasc Biol*. 2005;25(12):2542-2547. doi:10.1161/01.ATV.0000190701.92007.6d
28. Sumi M, Sata M, Toya N, Yanaga K, Ohki T, Nagai R. Transplantation of adipose stromal cells, but not mature adipocytes, augments ischemia-induced angiogenesis. *Life Sci*. 2007;80(6):559-565. doi:10.1016/j.lfs.2006.10.020
29. Cho J, Kang M, Lee K. TGF- β 1-treated ADSCs-CM promotes expression of type I collagen and MMP-1, migration of human skin fibroblasts, and wound healing in vitro and in vivo. *Int J Mol Med*. 2010;26(6):901-906. doi:10.3892/ijmm_00000540
30. Hu L, Wang J, Zhou X, et al. Exosomes derived from human adipose mesenchymal stem cells accelerates cutaneous wound healing via optimizing the characteristics of fibroblasts. *Scientific Reports*. 2016;6(1):32993. doi:10.1038/srep32993
31. Koenen P, Spanholtz TA, Maegle M, et al. Acute and chronic wound fluids inversely influence adipose-derived stem cell function: molecular insights into impaired wound healing. *Int Wound J*. 2015;12(1):10-16. doi:10.1111/iwj.12039
32. Wang L, Hu L, Zhou X, et al. Exosomes secreted by human adipose mesenchymal stem cells promote scarless cutaneous repair by regulating extracellular matrix remodelling. *Sci Rep*. 2017;7(1):13321-x. doi:10.1038/s41598-017-12919-x

33. Shu W, Shu YT, Dai CY, Zhen QZ. Comparing the biological characteristics of adipose tissue-derived stem cells of different persons. *J Cell Biochem*. 2012;113(6):2020-2026. doi:10.1002/jcb.24070
34. El-Ftesi S, Chang EI, Longaker MT, Gurtner GC. Aging and diabetes impair the neovascular potential of adipose-derived stromal cells. *Plast Reconstr Surg*. 2009;123(2):475-485. doi:10.1097/PRS.0b013e3181954d08
35. Ren G, Peng Q, Emmersen J, Zachar V, Fink T, Porsborg SR. A Comparative Analysis of the Wound Healing-Related Heterogeneity of Adipose-Derived Stem Cells Donors. *Pharmaceutics*. 2022;14(10):2126. doi: 10.3390/pharmaceutics14102126. doi:10.3390/pharmaceutics14102126
36. Fraser JK, Wulur I, Alfonso Z, Zhu M, Wheeler ES. Differences in stem and progenitor cell yield in different subcutaneous adipose tissue depots. *Cytotherapy*. 2007;9(5):459-467. doi:10.1080/14653240701358460
37. Peng Q, Ren G, Xuan Z, et al. Distinct Dominant Lineage from In Vitro Expanded Adipose-Derived Stem Cells (ASCs) Exhibits Enhanced Wound Healing Properties. *Cells*. 2022;11(7):1236. doi: 10.3390/cells11071236. doi:10.3390/cells11071236
38. Thirumala S, Goebel WS, Woods EJ. Manufacturing and banking of mesenchymal stem cells. *Expert Opin Biol Ther*. 2013;13(5):673-691. doi:10.1517/14712598.2013.763925
39. Haack-Sørensen M, Follin B, Juhl M, et al. Culture expansion of adipose derived stromal cells. A closed automated Quantum Cell Expansion System compared with manual flask-based culture. *J Transl Med*. 2016;14(1):319-9. doi:10.1186/s12967-016-1080-9
40. Barckhausen C, Rice B, Baila S, et al. GMP-Compliant Expansion of Clinical-Grade Human Mesenchymal Stromal/Stem Cells Using a Closed Hollow Fiber Bioreactor. *Methods Mol Biol*. 2016;1416:389-412. doi:10.1007/978-1-4939-3584-0_23
41. Hanley PJ, Mei Z, Durett AG, et al. Efficient manufacturing of therapeutic mesenchymal stromal cells with the use of the Quantum Cell Expansion System. *Cytotherapy*. 2014;16(8):1048-1058. doi:10.1016/j.jcyt.2014.01.417
42. Mizukami A, de Abreu Neto MS, Moreira F, et al. A Fully-Closed and Automated Hollow Fiber Bioreactor for Clinical-Grade Manufacturing of Human Mesenchymal Stem/Stromal Cells. *Stem Cell Rev Rep*. 2018;14(1):141-143. doi:10.1007/s12015-017-9787-4
43. Lechanteur C, Baila S, Janssens M, et al. Large-Scale Clinical Expansion of Mesenchymal Stem Cells in the GMP-Compliant, Closed Automated Quantum® Cell Expansion System: Comparison with Expansion in Traditional T-Flasks. *Journal of Stem Cell Research & Therapy*. 2014;04. doi:10.4172/2157-7633.1000222
44. BD Biosciences. Introduction to Flow Cytometry: A Learning Guide. 2002
45. McKinnon KM. Flow Cytometry: An Overview. *Curr Protoc Immunol*. 2018;120:5.1.1-5.1.11. doi:10.1002/cpim.40
46. Holmberg-Thyden S, Grønnebæk K, Gang AO, El Fassi D, Hadrup SR. A user's guide to multicolor flow cytometry panels for comprehensive immune profiling. *Anal Biochem*. 2021;627:114210. doi:10.1016/j.ab.2021.114210
47. Roederer M. Compensation in Flow Cytometry. *Current Protocols in Cytometry*. 2002;22(1):1.14.1-1.14.20. doi:10.1002/0471142956.cy0114s22
48. Carpentier G, Berndt S, Ferratge S, et al. Angiogenesis Analyzer for ImageJ — A comparative morphometric analysis of “Endothelial Tube Formation Assay” and “Fibrin Bead Assay”. *Scientific Reports*. 2020;10(1):11568. doi:10.1038/s41598-020-67289-8
49. Anderson P, Carrillo-Gálvez AB, García-Pérez A, Cobo M, Martín F. CD105 (endoglin)-negative murine mesenchymal stromal cells define a new multipotent subpopulation with distinct differentiation and immunomodulatory capacities. *PLoS One*. 2013;8(10):e76979. doi:10.1371/journal.pone.0076979
50. Russell KC, Phinney DG, Lacey MR, Barrilleaux BL, Meyertholen KE, O'Connor KC. In vitro high-capacity assay to quantify the clonal heterogeneity in trilineage potential of mesenchymal stem cells reveals a complex hierarchy of lineage commitment. *Stem Cells*. 2010;28(4):788-798. doi:10.1002/stem.312
51. Li X, Guo W, Zha K, et al. Enrichment of CD146(+) Adipose-Derived Stem Cells in Combination with Articular Cartilage Extracellular Matrix Scaffold Promotes Cartilage Regeneration. *Theranostics*. 2019;9(17):5105-5121. doi:10.7150/thno.33904
52. Álvarez-Viejo M, Menéndez-Menéndez Y, Otero-Hernández J. CD271 as a marker to identify mesenchymal stem cells from diverse sources before culture. *World J Stem Cells*. 2015;7(2):470-476. doi:10.4252/wjsc.v7.i2.470
53. Cuevas-Díaz Duran R, González-Garza MT, Cardenas-Lopez A, Chavez-Castilla L, Cruz-Vega DE, Moreno-Cuevas JE. Age-related yield of adipose-derived stem cells bearing the low-affinity nerve growth factor receptor. *Stem Cells Int*. 2013;2013:372164. doi:10.1155/2013/372164
54. Quirici N, Scavullo C, de Girolamo L, et al. Anti-L-NGFR and -CD34 monoclonal antibodies identify multipotent mesenchymal stem cells in human adipose tissue. *Stem Cells Dev*. 2010;19(6):915-925. doi:10.1089/scd.2009.0408
55. Mahmoud M, Juntunen M, Adnan A, et al. Immunomodulatory Functions of Adipose Mesenchymal Stromal/Stem Cell Derived From Donors With Type 2 Diabetes and Obesity on CD4 T Cells. *Stem Cells*. 2023;41(5):505-519. doi:10.1093/stmcls/sxad021
56. Levi B, Wan DC, Glotzbach JP, et al. CD105 protein depletion enhances human adipose-derived stromal cell osteogenesis through reduction of transforming growth factor β 1 (TGF- β 1) signaling. *J Biol Chem*. 2011;286(45):39497-39509. doi:10.1074/jbc.M111.256529
57. Yoshimura K, Shigeura T, Matsumoto D, et al. Characterization of freshly isolated and cultured cells derived from the fatty and fluid portions of liposuction aspirates. *J Cell Physiol*. 2006;208(1):64-76. doi:10.1002/jcp.20636
58. Mitchell JB, McIntosh K, Zvonick S, et al. Immunophenotype of human adipose-derived cells: temporal changes in stromal-associated and stem cell-associated markers. *Stem Cells*. 2006;24(2):376-385. doi:10.1634/stemcells.2005-0234
59. Newman PJ, Berndt MC, Gorski J, et al. PECAM-1 (CD31) cloning and relation to adhesion molecules of the immunoglobulin gene superfamily. *Science*. 1990;247(4947):1219-1222. doi:10.1126/science.1690453
60. ROBB KP, FITZGERALD JC, BARRY F, VISWANATHAN S. Mesenchymal stromal cell therapy: progress in manufacturing and assessments of potency. *Cytotherapy*. 2019;21(3):289-306. doi:10.1016/j.jcyt.2018.10.014